CONCISE ARTICLE

Triazole containing novobiocin and biphenyl amides as Hsp90 C-terminal inhibitors†

Jinbo Zhao,[a] Huiping Zhao,[a] Jessica A. Hall,[a] Douglas Brown,[d] Eileen Brandes,[b] Joseph Bazzill,[c] Patrick T. Grogan,[be] Chitra Subramanian,[b] George Vielhauer,[d] Mark S. Cohen[bce] and Brian S. J. Blagg*[a]

Hsp90 C-terminal inhibitors are advantageous for the development of new cancer chemotherapeutics due to their ability to segregate client protein degradation from induction of the prosurvival heat shock response, which is a major detriment associated with Hsp90 N-terminal inhibitors under clinical investigation. Based upon prior SAR trends, a 1,2,3-triazole side chain was placed *in lieu* of the aryl side chain and attached to both the coumarin and biphenyl scaffold. Antiproliferative studies against SKBr3 and MCF-7 breast cancer cell lines demonstrated these triazole-containing compounds to exhibit improved activity. These compounds were shown to manifest Hsp90 inhibitory activity through Western blot analysis and represent a new scaffold upon which more potent inhibitors can be pursued.

Introduction

Developments in molecular biology have led to identification of new targets for the pursuit of cancer chemotherapies during recent decades. The most successful demonstration thus far is Gleevec, a small molecule BCR/ABL kinase inhibitor used for the treatment of chronic myelogenous leukemia.[1,2] Due to their genetic instability and signaling redundancy, cancer cells exhibit compensatory mechanisms and often acquire resistance to inhibition of a single protein.[3] The most common approach to overcome this obstacle relies upon combination therapy, in which inhibitors of multiple oncogenic targets are administered. In contrast, the development of anti-cancer agents that target signaling nodes represent an alternative method to target multiple signaling pathways simultaneously while minimizing the potential for resistance.[4,5] The 90 kDa heat shock protein (Hsp90) represents a paradigmatic target for the latter approach, as molecular chaperones are responsible for the conformational maturation of signaling proteins associated with cancer cell growth and proliferation.[6,7] In fact, recent studies indicated that almost 400 Hsp90-depedent client proteins have been identified,[8,9] many of which are directly associated with the six hallmarks of cancer.[10] Consequently, Hsp90 inhibition results in the simultaneous disruption of multiple signaling pathways required for the viability of transformed cells. 17-AAG is a semi-synthetic derivative of geldanamycin that targets the N-terminal ATP-binding site and exhibits therapeutic benefit at tolerable doses in the clinic. In addition to 17-AAG, 16 other Hsp90 N-terminal inhibitors have been investigated in the clinical setting, which highlights the importance of Hsp90 as a cancer therapeutic target.[11] Unfortunately, these Hsp90 N-terminal inhibitors induce the pro-survival heat shock response at the same concentration needed to induce client protein degradation, resulting in primarily cytostatic activity. Thus, the clinical effectiveness of Hsp90 N-terminal inhibitors remains unclear.[12] In contrast to N-terminal inhibitors, studies have demonstrated that inhibitors of the Hsp90 C-terminus[13] and some allosteric modulators[14,15] do not induce the heat shock response, and consequently provide an attractive paradigm for the development of Hsp90 inhibitors that exhibit improved activities.[16,17]

Seminal work by Neckers and coworkers reported that the DNA gyrase inhibitor, novobiocin (**1**), and related natural products bind the Hsp90 C-terminus nucleotide binding pocket with low affinity (IC$_{50}$ ∼ 700 μM).[18] Subsequent modification to novobiocin including alteration of coumarin scaffold, optimization of the benzamide side chain, and replacement of the sugar moiety led to compounds that manifest increased inhibitory activity.[19–24] Although no co-crystal structure of Hsp90 bound to C-terminal inhibitors has been solved, insights gained from SAR studies on novobiocin has produced valuable information on the Hsp90 C-terminal binding pocket. Among the key elements on novobiocin identified, the secondary amide linker

[a] Department of Medicinal Chemistry, The University of Kansas, 1251 Wescoe Hall Drive, Malott 4070, Lawrence, Kansas 66045, USA. E-mail: bblagg@ku.edu; Fax: +1-785-864-5326; Tel: +1-785-864-2288

[b] Departments of Surgery, University of Michigan, Ann Arbor, MI, 48109, USA

[c] Pharmaceutical Chemistry, University of Michigan, Ann Arbor, MI, 48109, USA

[d] Departments of Urology, The University of Kansas Medical Center, 3901 Rainbow Blvd., Mail Stop 1016, Kansas City, KS 66160, USA

[e] Departments of Pharmacology, Toxicology and Therapeutics, The University of Kansas Medical Center, 3901 Rainbow Blvd., Mail Stop 1016, Kansas City, KS 66160, USA

† Electronic supplementary information (ESI) available. See DOI: 10.1039/c4md00102h

This journal is © The Royal Society of Chemistry 2014

Med. Chem. Commun., 2014, **5**, 1317–1323 | **1317**

and an aryl side chain were shown to be particularly important (Fig. 1A).[9] Structural modification to these moieties has produced analogues that exhibit improved activity, such as compound **2**, which contains a simplified coumarin core, a piperidine moiety, and a benzamide side chain (Fig. 1B). Increasing evidence suggests that hydrogen bonding interactions on the side chain are also beneficial,[21] which is in accord with the improved activities observed for analogues possessing a 2-[21] or 3-indole[25] or a 4-methoxyphenyl[23] side chain. Therefore, it was proposed that incorporation of additional hydrogen bonding interactions could further increase inhibitory activity. In addition, it was recently demonstrated that the coumarin core could be replaced with simplified surrogates,[26] which is imperative, due to the multi-step synthesis required for the preparation of this ring system. Indeed, replacement of the coumarin ring (**2**) system with a biphenyl scaffold (**3**) resulted in compounds that manifest increased antiproliferative activity (Fig. 1B).[27] Therefore, it was proposed that incorporation of a hydrogen bonding ring system onto both the coumarin and biphenyl scaffold could provide compounds that exhibit improved activity. Through exploratory methods, it was determined that the 1,2,3-triazole moiety represents an optimal side chain surrogate for the benzamide side chain present in novobiocin.

The copper catalyzed azido alkyne cycloaddition (CuAAC) reaction has found wide application to various fields of chemistry, especially biomedical and medicinal chemistry, due to the mild conditions required for assembly and its broad functional group tolerance.[28,29] The product obtained from such reactions, the 1,2,3-triazole, is an amide bioisostere that demonstrates enhanced hydrogen bonding interactions compared to the amide. In addition, the triazole ring is present in various therapeutic classes due to its hydrogen bonding capabilities and high dipole.[29,30] Prior studies have shown that bioisosteric

replacement of the amide linker on novobiocin with a 1,2,3-triazole resulted in decreased antiproliferative activity,[25] indicating that the amide N–H may be acting as a hydrogen bond donor. Therefore, it was proposed to incorporate the 1,2,3-triazole into the aryl side chain while retaining the secondary amide linker. To test this hypothesis, compounds **4** and **5** were designed to combine the features noted above, wherein the noviose sugar was replaced with a readily available piperidine moiety (Fig. 1C).[22] The results from these studies are presented herein and describe the identification of compounds that manifest mid-nanomolar activity, which is ~1000 fold more efficacious than novobiocin.

Results and discussion

Retrosynthetically, coumarin derivative **4** was envisioned for assembly by an amide coupling reaction between aniline **6** and triazolic acid **7**, with the latter being accessed through a CuAAC reaction between the corresponding azides and propiolic acid (Scheme 1). Synthesis of both the phenyl and benzyl derivatives (**4a** and **4b**) commenced by preparation of **7a** and **7b** from propiolic acid and the corresponding azides.[31] Aminocoumarin **6** was prepared via reported procedures.[22] Upon treatment with oxalyl chloride, triazolic acids **7a** and **7b** were converted to the corresponding acid chlorides and coupled with aminocoumarin **6** to provide **4a** and **4b** (Scheme 2).

The cellular activity manifested by **4a** and **4b** was evaluated against a panel of cancer lines (see ESI† for details), including SKBr3 (estrogen receptor negative, Her2 over-expressing) lymphatic metastatic MDA-MB-468LN (estrogen receptor negative, Ah receptor-positive) and MCF-7 (estrogen receptor positive) breast cancer cell lines, head and neck squamous cell carcinoma (HNSCC) MDA1986 and JMAR cell lines, as well as prostate cancer cell lines PC3-MM2 and LNCaP. Both
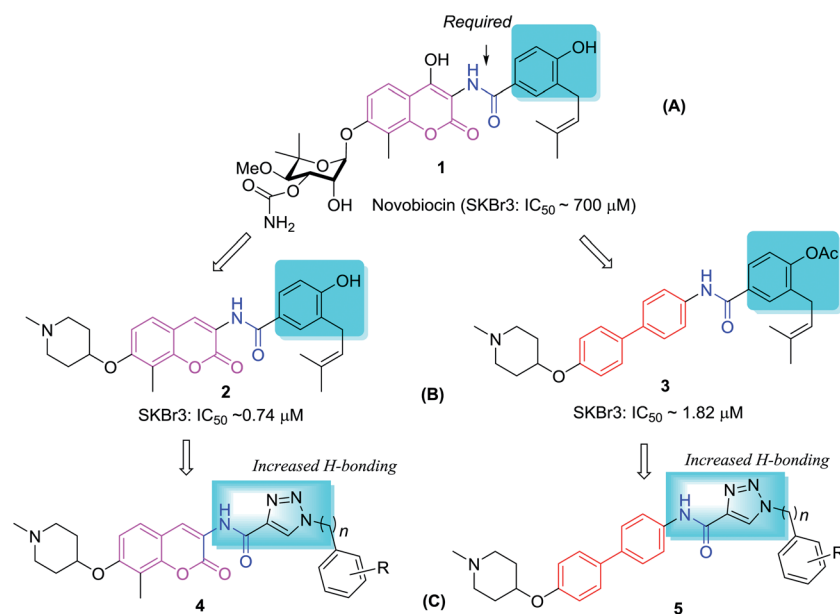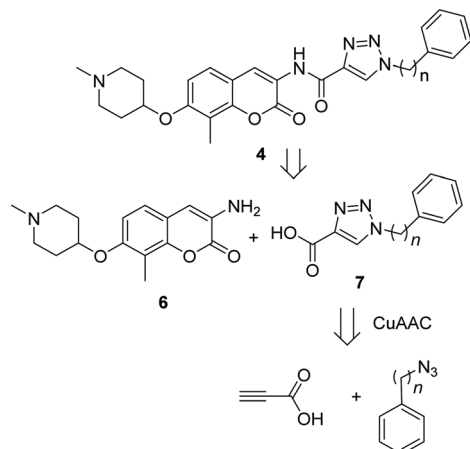

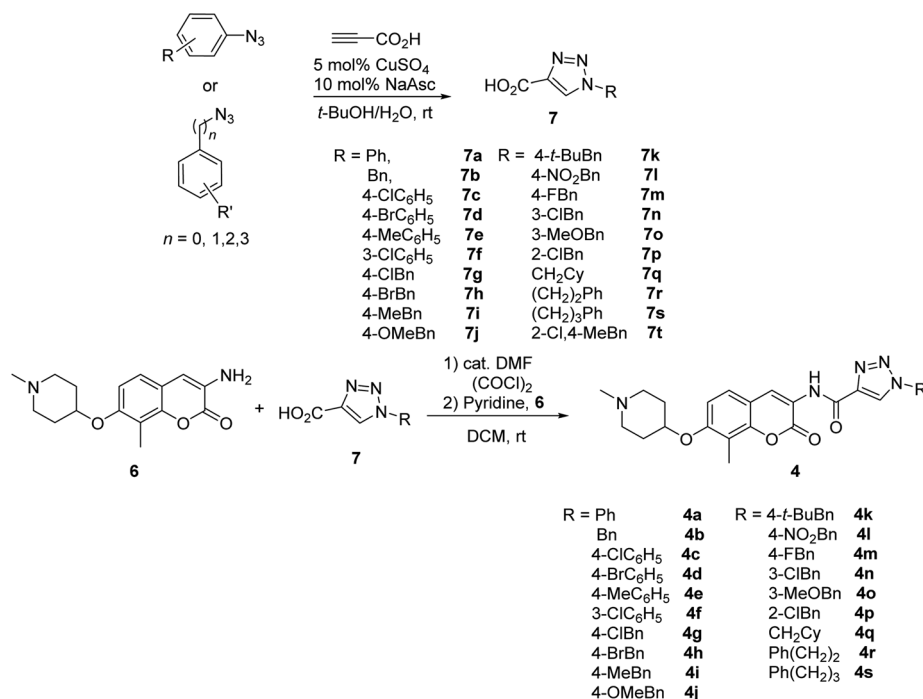Fig. 1 The design of novel Hsp90 C-terminal inhibitors.

Scheme 1 Retrosynthetic analysis of the triazole **4**.

compounds manifested activity at low micromolar concentrations against all cell lines tested. Encouraged by these preliminary studies, substitutions on the phenyl and benzyl side chains were explored to determine structure–activity relationships for this series of compounds. Compounds **4c–q** were synthesized efficiently in a manner similar to **4a** and **4b**, from the substituted triazolic acids **7c–q** and aniline **6** (Scheme 2). It was determined that both 4-chloro (**4c**) and 3-chloro (**4f**) substitutions improved inhibitory activity against SKBr3 cell lines. Due to comparable activities manifested by both the phenyl and benzyl analogues, studies were directed towards modification of the benzyl ring system. Electron-donating groups such as 4-methyl (**4i**) and 4-methoxy (**4j**) as well as 4-

chloro analogues (**4g**) manifested similar potencies compared to the unsubstituted analogue, **4b**. However, the 4-NO$_2$ substituent (**4l**) exhibited improved activity against all cancer cell lines tested, manifesting an IC$_{50}$ of 0.38 and 0.64 μM against SKBr3 and MCF-7 cell lines, respectively. Sterically bulky groups such as 4-*tert*-butyl (**4k**) were found favorable, although their effects on the MCF-7 cell line were not clear. When a hydrophobic cyclohexylmethyl group was installed as the appendage (**4q**), improved inhibitory activities against SKBr, MDA1986 and JMAR cells were observed, indicating the existence of a hydrophobic region in this area of the binding pocket. Although current data is limited and warrants further investigation, the observed inhibitory activities manifested by these triazole-containing analogues indicate that hydrogen bonding interactions on the side chain are favorable for Hsp90 C-terminal inhibition, which might result from either direct hydrogen bonding interactions or conformational rigidity on the side chain which might direct hydrophobic substituent into the hydrophobic pocket.

Increasing flexibility between the triazole side chain and the terminal phenyl ring was sought to determine whether improved inhibitory activity could be achieved. Therefore, compounds bearing two (**4r**) or three carbons (**4s**) were synthesized by an amide coupling reaction between the corresponding triazolylic acids (**7r** and **7s**) and amine **6** (Scheme 2). The antiproliferative activities manifested by these compounds were then determined. A comparison of the data shown for **4a,b** and **4r,s** (Table 1) illustrates that compound **4r**, which contains a two carbon linker, exhibited the most improved activity amongst the four analogues evaluated, exhibiting IC$_{50}$s of

Scheme 2 Synthesis of triazole containing coumarin derivatives.

This journal is © The Royal Society of Chemistry 2014

Med. Chem. Commun., 2014, **5**, 1317–1323 | **1319**

Table 1 Antiproliferative activity of coumarin-based triazole derivatives **4**[a]

R (4, IC$_{50}$, μM)	SKBr3[b]	MCF-7[b]	MDA-MB-468LN[c]	MDA1986[c]	JMAR[c]	PC3-MM2[d]	LNCaP[d]
Ph (**4a**)	0.94 ± 0.02[a]	1.33 ± 0.13[a]	1.10 ± 0.21	1.50 ± 3.40	2.30 ± 0.40	2.69	4.72 ± 0.71
Bn (**4b**)	0.99 ± 0.08	1.08 ± 0.00	2.40	1.60 ± 0.21	2.10 ± 0.23	9.8 ± 13.5	15.5 ± 8.75
4-ClC$_6$H$_5$ (**4c**)	0.58 ± 0.03	2.04 ± 0.25	0.81 ± 0.15	0.18 ± 0.11	0.43 ± 0.38	2.79 ± 0.49	2.45 ± 0.47
4-BrC$_6$H$_5$ (**4d**)	1.38 ± 0.05	5.07 ± 1.86	2.80 ± 0.50	2.90 ± 0.33	3.60 ± 0.63	3.81 ± 4.99	15.2 ± 9.19
4-MeC$_6$H$_5$ (**4e**)	1.08 ± 0.05	1.38 ± 0.07	4.00 ± 1.92	0.29	3.64	>100	>100
3-ClC$_6$H$_5$ (**4f**)	0.71 ± 0.14	1.14 ± 0.18	4.60	6.40	6.40	3.90 ± 5.11	13.3 ± 11.9
4-ClBn (**4g**)	1.14 ± 0.19	1.44 ± 0.31	2.20 ± 0.30	1.70 ± 0.52	1.70 ± 0.20	3.67 ± 1.38	4.65 ± 0.71
4-BrBn (**4h**)	0.73 ± 0.01	1.36 ± 0.08	2.10 ± 0.60	2.00 ± 0.50	1.60 ± 0.31	3.80 ± 1.42	4.96 ± 0.67
4-MeBn (**4i**)	1.21 ± 0.07	1.50 ± 0.19	2.40 ± 0.25	1.50 ± 0.20	1.80 ± 0.95	7.32 ± 5.44	7.24 ± 1.02
4-MeOBn (**4j**)	1.31 ± 0.20	1.42 ± 0.14	3.40 ± 1.27	2.60 ± 0.30	6.70	7.85 ± 0.42	>100
4-t-BuBn (**4k**)	0.45 ± 0.03	1.22 ± 0.07	0.74 ± 0.22	0.34 ± 0.09	0.58 ± 0.14	2.37 ± 0.00	1.84 ± 0.00
4-NO$_2$Bn (**4l**)	0.38 ± 0.13	0.64 ± 0.01	0.81 ± 0.23	0.18 ± 0.08	0.26 ± 0.34	2.49 ± 0.32	1.28 ± 0.71
4-FBn (**4m**)	1.08 ± 0.01	1.34 ± 0.19	2.60 ± 6.12	1.77 ± 4.10	2.38 ± 5.38	8.82 ± 1.14	3.31 ± 0.00
3-ClBn (**4n**)	1.06 ± 0.01	1.68 ± 0.01	1.14 ± 1.17	0.23 ± 0.22	0.19 ± 0.10	6.00 ± 1.13	3.03 ± 0.05
3-MeOBn (**4o**)	1.15 ± 0.19	1.61 ± 0.06	2.69 ± 1.33	1.34 ± 0.31	1.49 ± 0.31	7.20 ± 0.15	3.49 ± 0.30
2-ClBn (**4p**)	1.30 ± 0.07	0.99 ± 0.08	2.10 ± 0.52	3.20 ± 1.37	3.70 ± 0.85	6.66 ± 5.44	>100
CH$_2$C$_6$H$_{13}$ (**4q**)	0.61 ± 0.00	1.29 ± 0.16	0.99 ± 0.24	0.24 ± 0.32	0.30 ± 0.26	3.13 ± 0.14	1.20 ± 0.06
Ph(CH$_2$)$_2$ (**4r**)	0.13 ± 0.01	0.55 ± 0.01	0.99 ± 0.10	0.11 ± 0.30	0.74 ± 0.86	1.40 ± 0.04	2.36 ± 0.53
Ph(CH$_2$)$_3$ (**4s**)	1.73 ± 0.05	1.65 ± 0.03	NT	NT	NT	NT	NT

[a] Values represent mean ± standard deviation for at least two separate experiments performed in triplicate. [b] Cellular activities were determined with MTS/PMS cell viability assay. [c] Cellular activities were determined with Promega CellTiter-Glo (CTG) luminescent assay. [d] Cellular activities were determined with sulforhodamine B assay.

130 nM against SKBr3 cell line and about 110 nM against MDA1986 cell line.

To confirm that the observed antiproliferative activities were resulting from Hsp90 inhibition, western blot analyses of Hsp90 client proteins in MCF-7 cell lysates were performed. Actin, whose maturation does not require the Hsp90 machinery, was used as a control. As shown in Fig. 2, Hsp90 client proteins Her2, Akt and Raf-1 were degraded upon exposure of **4f**, **4o** or **4q** at concentrations that mirror their anti-proliferative values, confirming that cell viability is directly linked to Hsp90 inhibition.

Attention was then shifted to determine whether the anti-proliferative activities of these derivatives were similar to those of the recently identified biphenyl ring system. Biphenyl aniline **8** was synthesized according to a previously reported procedure.[25] Similar to the coumarin derivatives, triazolylic acids
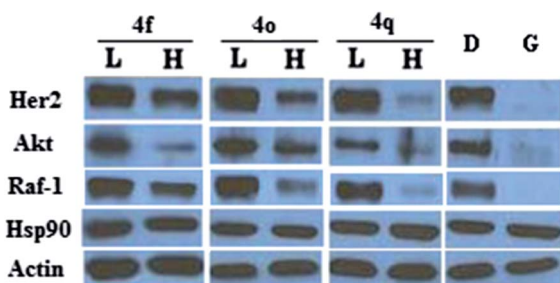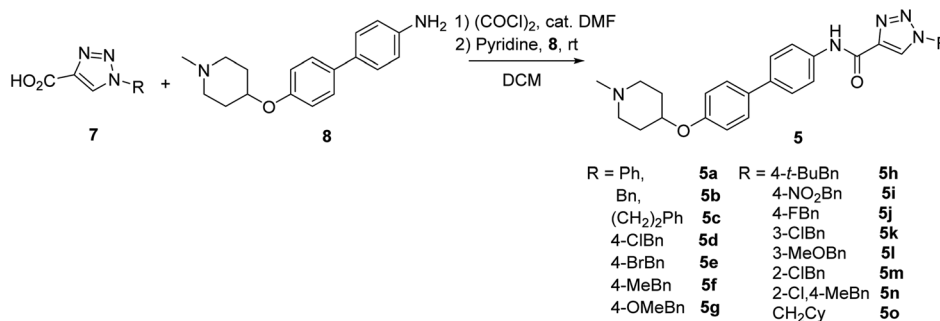

Fig. 2 Western blot analyses of the Hsp90 client protein degradation in MCF-7 breast cancer cells lysis after treatment of triazole analogues. L represents a concentration 1/2 of the anti-proliferative IC$_{50}$ value, while H represents a concentration 5 times the antiproliferative IC$_{50}$ value. Geldanamycin (G, 500 nM) represents a positive control, while DMSO (D), vehicle, serves as the negative control.

7a,b, **7g–q**, **7r** and **7t** were converted to their acid chlorides upon treatment with oxalyl chloride, followed by coupling with aniline **8** to generate the biphenyl containing derivatives **5a–o** (Scheme 3).

The antiproliferation activities manifested by these compounds are reported in Table 2. In contrast to the coumarin-based analogues **4a** and **4b**, which showed similar anti-proliferative activity, the phenyl and benzyl analogues **5a** and **5b** displayed very different activities, with the latter being about 2.5–8 times more potent against all the cell lines evaluated, manifesting IC$_{50}$s of 170 and 500 nM against SKBr3 and MCF-7 cell lines, respectively. A compound that contains the two carbon linker (**5c**) was found to exhibit activity similar to those of the benzyl analogue, **5b**. Subsequent studies were then aimed to modify the benzylic ring. As can be seen in Table 2, halogens at the 4-position were in general detrimental to inhibitory activity (**5d,e**); electron-donating groups such as 4-methyl (**5f**) and 4-methoxy (**5g**) retained potencies against SKBr3 and MDA-MB-468LN cells, but manifested increased inhibitory activities against the MCF-7 cell line (120 and 270 nM, respectively) and prostate cancer cell lines (360 and 480 nM, respectively). 3-Chloro (**5k**), 3-methoxy (**5l**), and 2-chloro (**5m**) produced decreased activity against SKBr3 cells, but increased activities against MCF-7 and MDA-MB-468LN cells. Combination of 2-chloro and 4-methyl substitution (**5n**) retained activity against SKBr3 cells, but did not improve activity against MCF-7 cells compared to the 4-methyl substituted analogue, **5f**. However, this combination indeed improved activities against MDA-MB-468LN, MDA1986 and LNCaP cell lines. Of particular note, the 4-tert-butyl substituted analogue, **5h**, manifested decreased antiproliferative activity against all cell lines tested compared to the 4-methyl analogue, **5f**, which is in contrast to

1320 | *Med. Chem. Commun.*, 2014, **5**, 1317–1323

This journal is © The Royal Society of Chemistry 2014

Scheme 3 Synthesis of biphenyl triazole derivatives **5**.

Table 2 Antiproliferative activity of biphenyl triazole analogues **5**[a]

R (5, IC$_{50}$, μM)	SKBr3[b]	MCF-7[b]	MDA-MB-468LN[c]	MDA1986[c]	JMAR[c]	PC3-MM2[d]	LNCaP[d]
Ph (5a)	1.14 ± 0.10[a]	1.44 ± 0.18[a]	0.83 ± 0.16	1.30 ± 0.09	2.20 ± 0.24	4.26 ± 5.59	3.89 ± 1.09
Bn (5b)	0.17 ± 0.02	0.50 ± 0.02	0.34 ± 0.07	0.28 ± 0.10	0.50 ± 0.06	0.55 ± 0.46	0.65 ± 0.54
CH$_2$Bn (5c)	0.19 ± 0.02	0.38 ± 0.10	0.36 ± 0.04	0.10 ± 0.23	0.58 ± 0.46	0.83 ± 0.34	0.43 ± 0.22
4-ClBn (5d)	0.32 ± 0.10	0.44 ± 0.04	0.74 ± 0.19	1.30 ± 0.37	2.30 ± 0.82	0.66 ± 0.21	1.59 ± 0.78
4-BrBn (5e)	0.49 ± 0.03	0.56 ± 0.04	2.80 ± 0.61	3.10 ± 0.87	7.80	19.9 ± 27.9	0.54 ± 0.12
4-MeBn (5f)	0.17 ± 0.03	0.12 ± 0.01	0.41 ± 0.26	0.36 ± 0.05	0.42 ± 0.07	0.36 ± 0.04	0.20 ± 0.04
4-MeOBn (5g)	0.16 ± 0.02	0.27 ± 0.06	0.17	0.48 ± 0.09	0.61 ± 0.09	0.44 ± 0.19	0.24 ± 0.07
4-t-BuBn (5h)	3.72 ± 0.68	10.48 ± 0.40	2.61 ± 0.76	2.34 ± 1.81	3.49 ± 2.05	>100	1.01 ± 1.39
4-NO$_2$ (5i)	0.45 ± 0.04	0.55 ± 0.01	0.56 ± 0.25	0.19 ± 0.17	0.21 ± 0.35	1.03 ± 0.16	0.60 ± 0.34
4-FBn (5j)	0.72 ± 0.18	1.04 ± 0.08	1.09 ± 0.23	0.93 ± 0.34	1.39 ± 0.52	2.81 ± 1.82	1.64 ± 0.97
3-ClBn (5k)	0.39 ± 0.01	0.34 ± 0.02	0.17 ± 0.02	0.17 ± 0.12	0.27 ± 0.04	0.35 ± 0.14	0.12 ± 0.10
3-MeOBn (5l)	0.32 ± 0.02	0.16 ± 0.02	0.19 ± 0.05	0.28 ± 0.09	0.21 ± 0.12	0.55 ± 0.37	0.16
2-ClBn (5m)	0.34 ± 0.04	0.38 ± 0.03	0.22 ± 0.03	0.81 ± 0.05	0.65	1.04 ± 0.51	0.61 ± 0.34
2-Cl,4-MeBn (5n)	0.16 ± 0.01	0.20 ± 0.05	0.15 ± 0.02	0.15 ± 0.06	0.43 ± 0.25	0.35 ± 0.12	0.05 ± 0.04
CH$_2$C$_6$H$_{13}$ (5o)	0.20 ± 0.02	0.31 ± 0.04	0.24 ± 0.06	0.38 ± 0.14	0.26 ± 0.45	5.12 ± 6.54	0.48 ± 0.68

[a] Values represent mean ± standard deviation for at least two separate experiments performed in triplicate. [b] Cellular activities were determined with MTS/PMS cell viability assay. [c] Cellular activities were determined with Promega CellTiter-Glo (CTG) luminescent assay. [d] Cellular activities were determined with sulforhodamine B assay.

the coumarin derivatives **4i** and **4k**, indicating a smaller hydrophobic pocket exists when the biaryl scaffold is present. Similar to the coumarin scaffold, replacement of the benzyl group with a cyclohexylmethyl substituent resulted in compounds that manifested good inhibitory activities. Differences in the structure–activity relationships for the two scaffolds suggest the biphenyl ring system presents the side chain through different binding interactions. In general, installation of triazole side chain on the recently identified biphenyl side chain greatly improves antiproliferative activity against a wide spectrum of cell lines, resulting in more potent analogues.

The cellular activity manifested by these biphenyl analogues was shown to result from Hsp90 inhibition by performing western blot analyses of MCF-7 cell lysates treated with such compounds. Hsp90-dependent client proteins were decreased upon exposure to of **5b**, **5f** and **5g** at concentrations that mirror their antiproliferative IC$_{50}$s. Clear degradation of Hsp90 client proteins Her2, Akt and Raf-1 was observed, while actin, which does not rely upon the Hsp90 chaperone machinery, remained constant, indicating that the antiproliferative activities manifested by these compounds resulted from Hsp90 inhibition (Fig. 3A). These client proteins Her2, Akt, Raf-1 and CDK6 were

also degraded in a concentration-dependent manner upon exposure to the most potent analogue **5f** and the representative analogue **5b**, against MCF-7 cells (Fig. 3B and C), while actin levels remain unchanged. Examination of Hsp90 expression when exposed to these compounds have shown that while GDA, the positive control, induced Hsp90 upregulation due to induced heat shock response, Hsp90 levels were constant or even decreased upon treatment of these compounds (Fig. 3), consistent with the observations manifested by many Hsp90 C-terminal inhibitors,[20,22,24,27,32] indicating that these compounds exhibit Hsp90 inhibitory activity through C-terminal inhibition. It is worthwhile to note that at a concentration as low as 1 μM, **5f** was able to deplete Hsp90 client proteins as well as Geldanamycin at 500 nM, demonstrating the remarkable activity exhibited by this compound for Hsp90 inhibition.

Furthermore, no increase in heat shock proteins Hsp27, Hsp70, or Hsp90 was observed with increasing concentrations of **5f** (Fig. 4A). Depletion of client proteins without increased levels of heat shock proteins is a hallmark of Hsp90 C-terminal inhibition. To determine whether **5f** binds the Hsp90 C-terminus, proteolytic fingerprinting of Hsp90 from TnT rabbit reticulocyte in the presence of **5f** was performed. Novobiocin
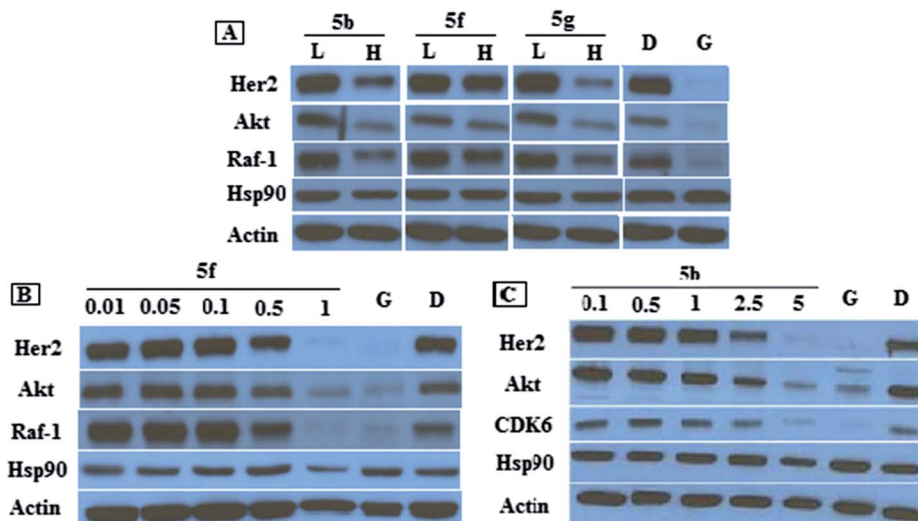
This journal is © The Royal Society of Chemistry 2014

Med. Chem. Commun., 2014, **5**, 1317–1323 | **1321**

Fig. 3 Western blot analyses of the Hsp90 client protein degradation in MCF-7 breast cancer cells lysis 24 h after treatment of biphenyl triazole analogues **5b**, **5f** and **5g**. (A) L represents a concentration 1/2 of the anti-proliferative IC_{50} value, while H represents a concentration 5 times the antiproliferative IC_{50} value. (B) Concentrations (in µM) of **5f** are indicated above each lane. (C) Concentrations of **5b** (in µM) are indicated above each lane. Geldanamycin (G, 500 nM) and DMSO (D) were employed respectively as positive and negative controls.
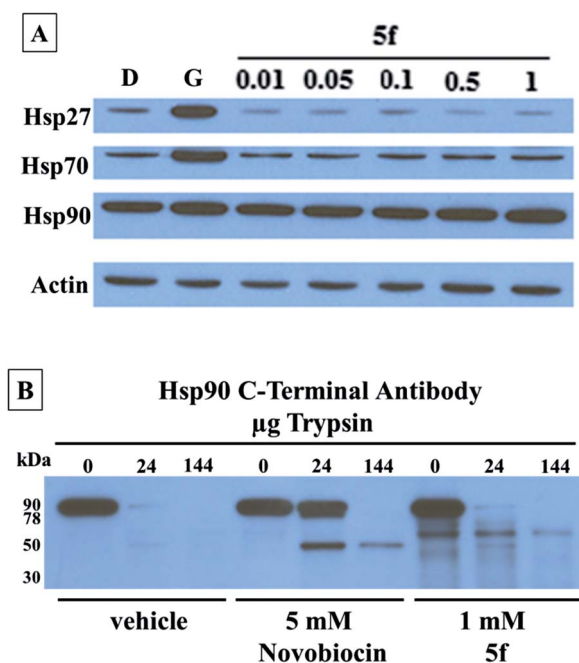

Fig. 4 (A) Western blot analyses of the heat shock proteins Hsp27, Hsp70 and Hsp90 in MCF-7 breast cancer cells lysates 24 h after treatment with **5f**. Concentrations (in µM) of **5f** are indicated above each lane. Geldanamycin (G, 500 nM) and DMSO (D) are positive and negative controls. (B) Proteolysis of Hsp90 from TnT reticulocyte lysate incubated under conditions of protein synthesis with vehicle (1% DMSO) 5 mM novobiocin and 1 mM **5f**. An antibody specific to the C-terminus of Hsp90 was used to identify the Hsp90 fragments produced in the presence of increasing amounts of trypsin.

molecular weight from vehicle control. The C-terminal Hsp90 antibody AC88 detects the emergence of a 50 kDa band in the presence of novobiocin and other C-terminal inhibitors. A 50 kDa band was detected with 5 mM novobiocin and 1 mM **5f** that is not detected for the vehicle control (Fig. 4B). Together, these data further support that **5f** binds and inhibits the Hsp90 C-terminus, which leads to client protein degradation without induction of the heat shock response.

A brief summary of observed structure–activity relationships for these derivatives is depicted in Fig. 5. In support of the existence a hydrophobic pocket, incorporation of either an aromatic or saturated carbocycle was found favorable to inhibitory activity. Two carbons were found optimal for the coumarin derivatives, compared to one carbon for the biphenyl derivatives; and suggests that projection of the side chain is different for the biaryl scaffold. This observation is further supported by the tolerance of bulky groups exhibited at the *para* position of benzylic moiety (**4k**), but not for the biphenyl derivative, **5h**. These observations highlight the significance of
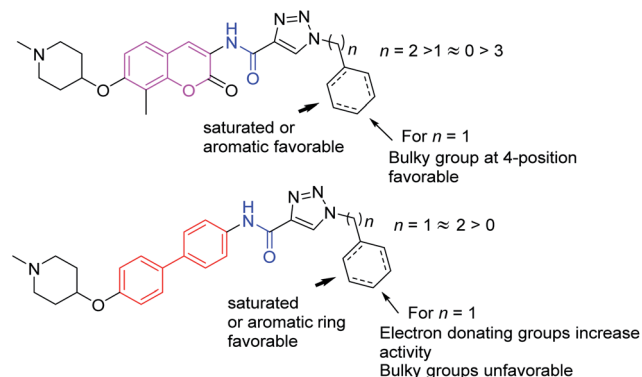
locks Hsp90 in the "open conformation" when bound to the C-terminus.[33,34] In this conformation, amino acids Lys615 and Arg620 are not solvent exposed and are "protected" from cleavage by trypsin. This results in bands that differ in

Fig. 5 A summary of SARs for triazole containing coumarin and biphenyl derivatives.

both hydrogen bonding and hydrophobic interactions at this location of the Hsp90 C-terminal binding pocket.

Conclusion

In conclusion, a series of 1,2,3-triazole side chain containing analogues that contain the coumarin or biphenyl backbone were designed, synthesized and evaluated for antiproliferative activities against a panel of breast, HNSCC, and prostate cancer cell lines. Compounds manifesting nanomolar activity were identified through preliminary SAR studies and their Hsp90 inhibitory activity confirmed by Western blot analysis. The improved Hsp90 inhibitory activities exhibited by these compounds might result from increased hydrogen bonding properties on the amide side chain when connected to a hydrophobic appendage, or from the conformational rigidity due to the incorporation of 1,2,3-triazole which directs the hydrophobic appendage into the hydrophobic pocket. These observations are expected to aid in the development of more potent Hsp90 C-terminal inhibitors, and such studies will be reported in due course.

Acknowledgements

References

1 X. An, A. K. Tiwari, Y. Sun, P.-R. Ding, C. R. Ashby, Jr and Z.-S. Chen, *Leuk. Res.*, 2010, **34**, 1255–1268.

2 M. Henkes, H. van der Kuip and W. E. Aulitzky, *Ther. Clin. Risk Manage.*, 2008, **4**, 163–187.

3 C. Roche-Lestienne and C. Preudhomme, *Hematologie*, 2007, **13**, 43–53.

4 X. Lu, L. Xiao, L. Wang and D. M. Ruden, *Biochem. Pharmacol.*, 2012, **83**, 995–1004.

5 K. Jhaveri and S. Modi, in *Advances in Pharmacology*, ed. S. M. S. Keiran, Academic Press, 2012, vol. 65, pp. 471–517.

6 P. Workman, F. Burrows, L. Neckers and N. Rosen, *Ann. N. Y. Acad. Sci.*, 2007, **1113**, 202–216.

7 B. S. J. Blagg and T. D. Kerr, *Med. Res. Rev.*, 2006, **26**, 310–338.

8 M. Taipale, I. Krykbaeva, M. Koeva, C. Kayatekin, K. D. Westover, G. I. Karras and S. Lindquist, *Cell*, 2012, **150**, 987–1001.

9 I. Fierro-Monti, P. Echeverria, J. Racle, C. Hernandez, D. Picard and M. Quadroni, *PLoS One*, 2013, **8**, e80425.

10 D. Hanahan and R. A. Weinberg, *Cell*, 2000, **100**, 57–70.

11 (*a*) M. A. Biamonte, R. Van de Water, J. W. Arndt, R. H. Scannevin, D. Perret and W.-C. Lee, *J. Med. Chem.*, 2010, **53**, 3–17; (*b*) Y. S. Kim, S. V. Alarcon, S. Lee, M. J. Lee, G. Giaccone, L. Neckers and J. B. Trepel, *Curr. Top. Med. Chem.*, 2009, **9**, 1479–1492.

12 C. K. Vaughan, L. Neckers and P. W. Piper, *Nat. Struct. Mol. Biol.*, 2010, **17**, 1400–1404.

13 J. D. Eskew, T. Sadikot, P. Morales, A. Duren, I. Dunwiddie, M. Swink, X. Zhang, S. Hembruff, A. Donnelly, R. A. Rajewski, B. S. J. Blagg, J. R. Manjarrez, R. L. Matts, J. M. Holzbeierlein and G. A. Vielhauer, *BMC Cancer*, 2011, **11**, 468.

14 J. M. McConnell, L. D. Alexander and S. R. McAlpine, *Bioorg. Med. Chem. Lett.*, 2014, **24**, 661–666.

15 V. C. Ardi, L. D. Alexander, V. A. Johnson and S. R. McAlpine, *ACS Chem. Biol.*, 2011, **6**, 1357–1367.

16 L. B. Peterson and S. J. Brian, *Future Med. Chem.*, 2009, **1**, 267–283.

17 H. Zhao and B. S. J. Blagg, Inhibitors of Molecular Chaperones as Therapeutic Agents, *RSC Drug Discovery Ser.*, 2014, 259–301.

18 M. G. Marcu, T. W. Schulte and L. Neckers, *J. Natl. Cancer Inst.*, 2000, **92**, 242.

19 X. M. Yu, G. Shen, L. Neckers, H. Blake, J. Holzbeierlein, B. Cronk and B. S. J. Blagg, *J. Am. Chem. Soc.*, 2005, **127**, 12778–12779.

20 J. A. Burlison, L. Neckers, A. B. Smith, A. Maxwell and B. S. J. Blagg, *J. Am. Chem. Soc.*, 2006, **128**, 15529–15536.

21 J. A. Burlison, C. Avila, G. Vielhauer, D. J. Lubbers, J. Holzbeierlein and B. S. J. Blagg, *J. Org. Chem.*, 2008, **73**, 2130–2137.

22 H. P. Zhao, B. R. Kusuma and B. S. J. Blagg, *ACS Med. Chem. Lett.*, 2010, **1**, 311–315.

23 H. P. Zhao, A. C. Donnelly, B. R. Kusuma, G. E. L. Brandt, D. Brown, R. A. Rajewski, G. Vielhauer, J. Holzbeierlein, M. S. Cohen and B. S. J. Blagg, *J. Med. Chem.*, 2011, **54**, 3839–3853.

24 H. P. Zhao and B. S. J. Blagg, *Bioorg. Med. Chem. Lett.*, 2013, **23**, 552–557.

25 (*a*) L. B. Peterson and B. S. J. Blagg, *Bioorg. Med. Chem. Lett.*, 2010, **20**, 3957–3960; (*b*) H. P. Zhao, E. Moroni, G. Colombo and B. S. J. Blagg, *ACS Med. Chem. Lett.*, 2014, **5**, 84–88.

26 A. C. Donnelly, J. R. Mays, J. A. Burlison, J. T. Nelson, G. Vielhauer, J. Holzbeierlein and B. S. J. Blagg, *J. Org. Chem.*, 2008, **73**, 8901–8920.

27 H. P. Zhao, E. Moroni, G. Colombo and B. S. J. Blagg, *ACS Med. Chem. Lett.*, 2014, **5**, 84–88.

28 G. C. Tron, T. Pirali, R. A. Billington, P. L. Canonico, G. Sorba and A. A. Genazzani, *Med. Res. Rev.*, 2008, **28**, 278–308.

29 H. C. Kolb and K. B. Sharpless, *Drug Discovery Today*, 2003, **8**, 1128–1137.

30 P. Thirumurugan, D. Matosiuk and K. Jozwiak, *Chem. Rev.*, 2013, **113**, 4905–4979.

31 A. Kolarovic, M. Schnurch and M. D. Mihovilovic, *J. Org. Chem.*, 2011, **76**, 2613–2618.

32 B. R. Kusuma, A. Khandewal, W. Gu, D. Brown, W. Liu, G. Vielhauer, J. Holzbeierlein and B. S. J. Blagg, *Bioorg. Med. Chem.*, 2014, **22**, 1441–1449.

33 R. L. Matts, A. Dixit, L. B. Peterson, L. Sun, S. Voruganti, P. Kalyanaraman, S. D. Hartson, G. M. Verkhivker and B. S. J. Blagg, *ACS Chem. Biol.*, 2011, **6**, 800–807.

34 B.-G. Yun, W. Huang, N. Leach, S. D. Hartson and R. L. Matts, *Biochemistry*, 2004, **43**, 8217–8229.

This journal is © The Royal Society of Chemistry 2014

Med. Chem. Commun., 2014, **5**, 1317–1323 | **1323**